Title

Fluorescence Anisotropy-Based Tethering for Discovery of Protein–Protein Interaction Stabilizers

Journal

ACS Chemical Biology, 15(12)

ISSN

1554-8929

Authors

Sijbesma, Eline
Somsen, Bente A
Miley, Galen P
et al.

Publication Date

2020-12-18

DOI

10.1021/acschembio.0c00646

Peer reviewed

ACS chemical biology

pubs.acs.org/acschemicalbiology

Articles

Fluorescence Anisotropy-Based Tethering for Discovery of Protein–Protein Interaction Stabilizers

Eline Sijbesma,[‖] Bente A. Somsen,[‖] Galen P. Miley, Iris A. Leijten-van de Gevel, Luc Brunsveld, Michelle R. Arkin,* and Christian Ottmann*

Cite This: *ACS Chem. Biol.* 2020, 15, 3143–3148

Read Online

ACCESS | Metrics & More | Article Recommendations | Supporting Information

ABSTRACT: Protein–protein interaction (PPI) networks are fundamental for cellular processes. Small-molecule PPI enhancers have been shown to be powerful tools to fundamentally study PPIs and as starting points for potential new therapeutics. Yet, systematic approaches for their discovery are not widely available, and the design prerequisites of "molecular glues" are poorly understood. Covalent fragment-based screening can identify chemical starting points for these enhancers at specific sites in PPI interfaces. We recently reported a mass spectrometry-based disulfide-trapping (tethering) approach for a cysteine residue in the hub protein 14–3–3, an important regulator of phosphorylated client proteins. Here, we invert the strategy and report the development of a functional read-out for systematic identification of PPI enhancers based on fluorescence anisotropy (FA-tethering) with the reactive handle now on a client-derived peptide. Using the DNA-binding domain of the nuclear receptor Estrogen Related Receptor gamma (ERRγ), we target a native cysteine positioned at the 14–3–3 PPI interface and identify several fragments that form a disulfide bond to ERRγ and stabilize the complex up to 5-fold. Crystallography indicates that fragments bind in a pocket comprised of 14–3–3 and the ERRγ phosphopeptide. FA-tethering presents a streamlined methodology to discover molecular glues for protein complexes.

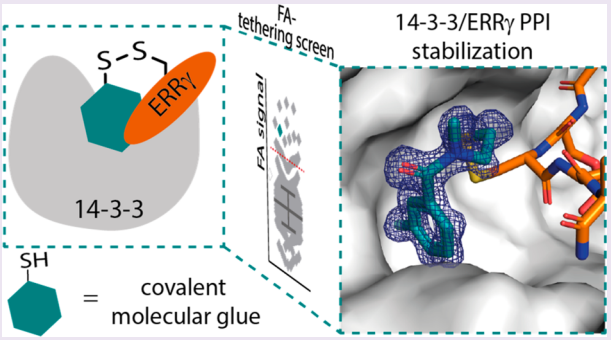

Physical interactions between proteins have increasingly been recognized as an attractive means to manipulate protein function. As such, small-molecule modulators of protein–protein interactions (PPIs) have become highly sought after.[1] By modulating their interactions with regulatory proteins, disease-related proteins that were previously regarded as "undruggable" targets have become tractable for therapeutic intervention.[2,3] Whereas most successes have been described for PPI inhibitors, great potential remains to be realized for enhancer molecules acting as "molecular glue" to stabilize protein complexes.[4,5] The discovery of such compounds has proved to be challenging, as apparent from the scarcity of systematic small-molecule PPI enhancers in the literature. Yet, examples of natural product PPI stabilizers[6,7] and the successes in using heterobifunctional probes for induced protein degradation (PROTACs)[8] strongly support the value of molecules with a PPI stabilization mode of action and the development of screening technologies for their rational discovery and design.

We are developing systematic PPI stabilization strategies for the family of host/client complexes involving the host protein 14–3–3. These adaptor proteins regulate the activity, cellular localization, and/or the stability of client proteins by binding to phosphorylated motifs in their sequence. The important and widespread chaperone function and the large number of cellular binding partners places 14–3–3 at critical nodes in disease-related signaling networks.[9,10]

Recently, we reported a fragment-based discovery strategy based on disulfide trapping ("tethering")[11,12] for the identification of molecular glues, resulting in hit molecules that stabilize the 14–3–3/Estrogen Receptor α (ERα) complex while tethered to a cysteine residue on the 14–3–3 host.[13] Herein, we demonstrate a variant of the tethering approach in which we target a native cysteine residue found in the 14–3–3 binding motif of the Estrogen Related Receptor gamma's DNA binding domain (ERRγ DBD). In this approach, the ERRγ-phosphopeptide is labeled with a fluorescent probe, and the fragment-induced binding of ERRγ-phosphopeptide to 14–3–3 is monitored by an increase in fluorescence anisotropy (FA; Figure 1). The use of FA-tethering as a functional readout has previously been established in campaigns to identify PPI disruptors for KIX

Received: August 10, 2020
Accepted: November 3, 2020
Published: November 16, 2020

https://dx.doi.org/10.1021/acschembio.0c00646
ACS Chem. Biol. 2020, 15, 3143–3148

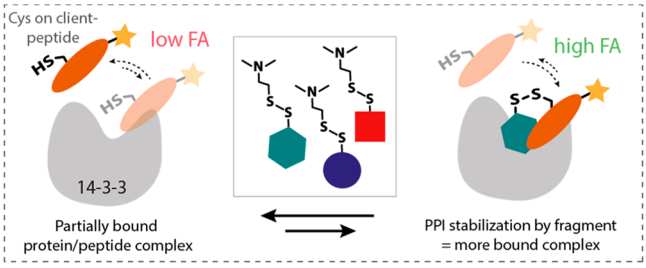

Figure 1. Schematic representation of FA-tethering for PPI stabilizers by fluorescence anisotropy (FA). A fluorescently labeled cysteine-containing client peptide is initially weakly bound to 14−3−3, as evidenced by low FA (low anisotropy). Stabilization of the protein−peptide complex upon incubation with a disulfide library, under reducing conditions, leads to increased 14−3−3 binding to the client peptide, observed by an increase in anisotropy.

and PDK1.[14,15] The new method, in which the fragment binds to the client peptide to enhance PPI complex formation, contrasts with the previously published screens in which PPI complex formation was inhibited. Taken together, FA-tethering is a rapid, functional assay for directly screening for PPI *inhibitors* and *stabilizers*.

NOVEL 14−3−3 INTERACTION MOTIFS IN A NUCLEAR RECEPTOR

Members of the nuclear receptor (NR) superfamily of ligand-responsive transcription factors are master regulators of specific target genes and are implicated in a range of pathological conditions.[16] On the basis of cellular and proteomics studies, several NRs have been hypothesized to be regulated by 14−3−3.[17−19] Whereas the phosphorylated 14−3−3 binding motif in ERα has been validated in cellular studies, most putative 14−3−3/NR interactions remain unvalidated, including for ERRγ, a relevant drug target in insulin metabolism.[19,20] The phosphorylation of ERRγ at S179 by protein kinase B (PKB) has been proposed to drive 14−3−3 binding, resulting in decreased nuclear localization[19] and providing endogenous inhibition of ERRγ activity by 14−3−3. Since the molecular mechanism for formation of this protein complex remains to be unraveled, we first focused on the biochemical and structural characterization of the 14−3−3/ERRγ interaction. In addition to the pS179 motif in the ERRγ DBD, a second motif in the ligand-binding domain (LBD) was identified by the 14−3−3 prediction tool developed by the MacKintosh and Barton groups.[21] Binding of both phosphorylated ERRγ motifs to the seven human 14−3−3 isoforms was confirmed by FA and isothermal calorimetry (ITC) studies (Figure 2a,b, SI Figure S1).

14−3−3/ERRγ PPI: A CYSTEINE IN A DRUGGABLE POCKET

To characterize these two 14−3−3/peptide binding interactions, we obtained highly diffracting cocrystal structures using the 14−3−3 sigma isoform (14−3−3σ). Crystals of 14−3−3σ bound by the ERRγ LBD or DBD motif diffracted to 1.9 and 1.4 Å, respectively. The electron density for the ERRγ LBD motif allowed modeling for five of eight peptide residues (SL{pS^{319}}FE; SI Figure S2). The electron density for the ERRγ DBD motif allowed seven amino acids of a 9-mer

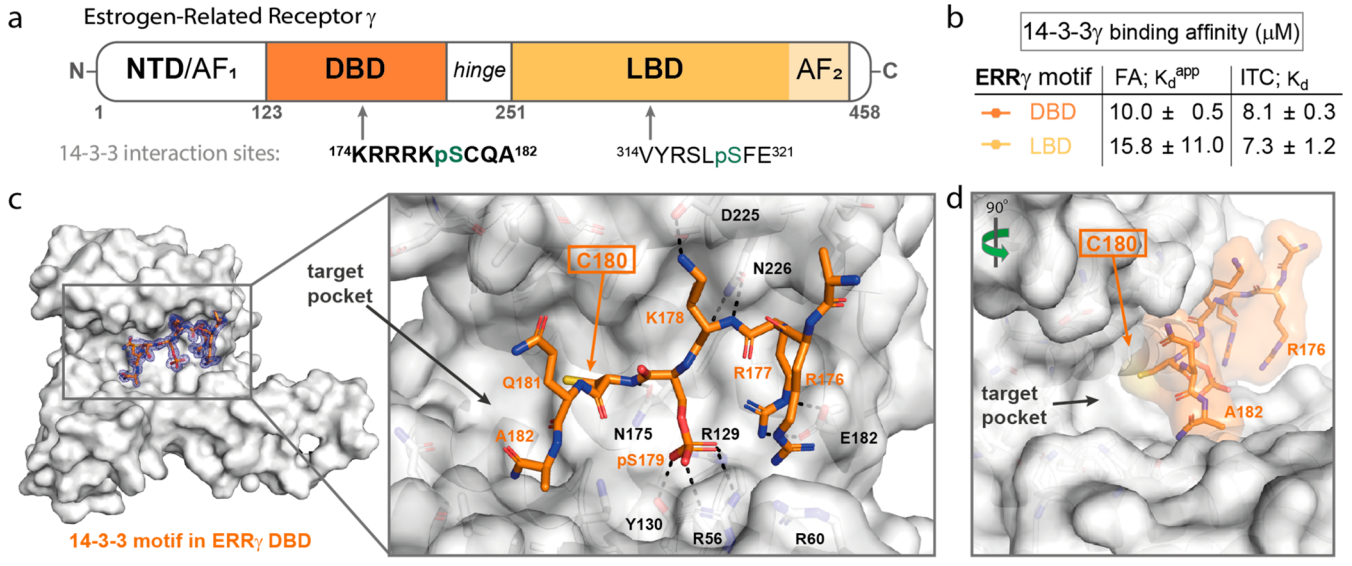

Figure 2. (a) Schematic representation of the ERRγ domain organization, including the N-terminal domain (NTD), DNA-binding domain (DBD), and ligand-binding domain (LBD). AF: activation function. The phosphorylated 14−3−3 interaction motifs studied in this work and their relative positions in the ERRγ protein sequence are indicated. (b) Validation of 14−3−3 binding affinity for the ERRγ DBD and LBD motifs, as determined by fluorescence anisotropy (FA) and isothermal titration calorimetry (ITC). (c) Co-crystal structure of 14−3−3σ bound by phosphorylated ERRγ DBD motif (PDB: 6Y1D). Front view of a 14−3−3 monomer (white surface) bound by ERRγ phosphopeptide (orange sticks) and close-up view of the peptide in the primary 14−3−3 binding groove (white cartoon and sticks representation). Polar contacts (black dashed lines) were observed between the phospho-group of S179 (ERRγ) and the Arg-Arg-Tyr triad R56, R129, and Y130 (14−3−3). N175 and N226 of 14−3−3 interact with the backbone of ERRγ's C180 and K178, respectively. Furthermore, one polar contact was observed between D225 (14−3−3) and K178 (ERRγ), and two polar contacts were observed between E182 (14−3−3) and the guanidinium of R177 (ERRγ). The guanidinium groups of R176, R177 (ERRγ), and R60 (14−3−3) form a triple stack. $2F_o - F_c$ electron density maps are contoured at 1σ. (d) Side view of 14−3−3σ (white surface) bound by ERRγ phosphopeptide (orange sticks with transparent surface) revealing a target pocket for 14−3−3/ERRγ DBD with C180 of the ERRγ peptide motif oriented toward it.

https://dx.doi.org/10.1021/acschembio.0c00646
ACS Chem. Biol. 2020, 15, 3143−3148

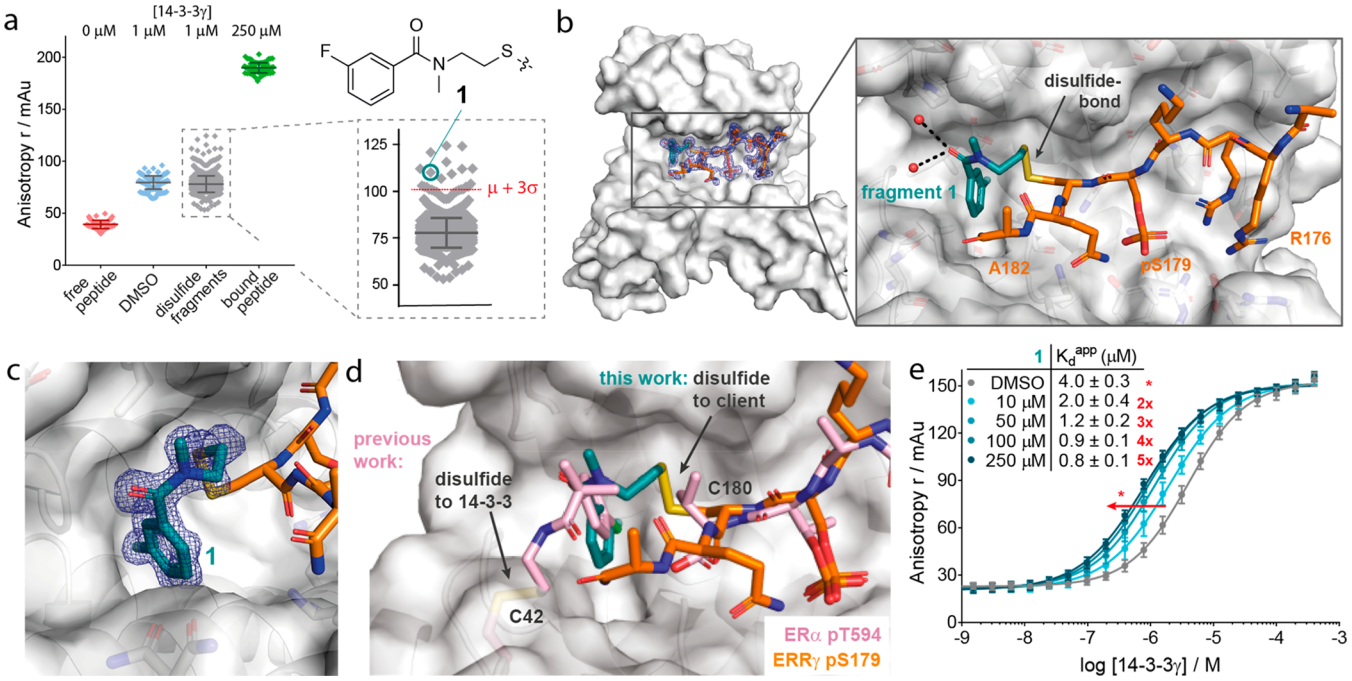

Figure 3. (a) FA-tethering screening results showing anisotropy values for fluorescently labeled ERRγ DBD phosphopeptide binding to 14−3−3γ. Anisotropy values for free peptide (0 μM 14−3−3γ, negative control) are shown in red and bound peptide (250 μM 14−3−3γ, positive control) in green. Screening data of individual disulfide fragments (gray) is obtained with 1 μM 14−3−3γ (~25% bound) with DMSO (blue) as control. Bars represent mean (μ) and standard deviation (σ). A hit selection cutoff value of μ + 3σ was used. Selected hit fragment **1** is indicated (blue circle). (b) Front view of a 14−3−3σ monomer (white surface) bound by ERRγ DBD phosphopeptide (orange sticks) with disulfide-bound **1** (turquoise sticks). Depicted are polar contacts (black dotted lines) and water molecules (red spheres). PDB: 6Y3W (c) Close-up view of ERRγ DBD-**1** in the 14−3−3 binding groove. $2F_o - F_c$ electron density maps are contoured at 1σ. (d) Crystallographic overlay of 14−3−3/ERRγ DBD (orange sticks) with ERRγ (C180)-trapped-**1** (teal sticks) and 14−3−3/ERα (pink sticks) with 14−3−3(C42)-trapped-stabilizer (pink sticks; PDB: 6HMT). (e) Dose−response anisotropy data for 14−3−3γ titrations to the ERRγ DBD phosphopeptide in the presence of increasing concentrations of **1**, with resulting apparent K_d values and fold stabilization in red.

phosphopeptide to be built (RRK{pS^{179}}CQA; Figure 2c). This ERRγ (pS179) peptide motif resides in the second zinc finger motif of the DBD, and C180 is a part of the Zn^{2+}-coordinating Cys_4 structural fold.[22] Interestingly, the cocrystal structure revealed that the cysteine residue (C180) at the +1 position with respect to the phosphorylated serine pointed directly into a pocket formed by the 14−3−3/peptide complex (Figure 2d). This orientation of C180 in the 14−3−3 binding groove inspired our efforts to discover disulfide-bound fragments to stabilize this complex.

DISULFIDE TRAPPING BY FA-TETHERING TO FIND STABILIZERS

We have previously shown that a natural or engineered cysteine residue in close proximity to a ligandable pocket can aid the discovery of PPI stabilizers through the use of disulfide trapping ("tethering").[11,13] This approach was demonstrated for the interaction of 14−3−3 with ERα,[13] where we incubated a cysteine-containing isoform of 14−3−3 with a disulfide-containing fragment library in the *apo* or phosphopeptide-bound state and quantified the protein-fragment conjugate by intact protein mass spectrometry (MS). We envisioned that an inversion of this paradigm, wherein a cysteine residue was located on the client-derived peptide, could also be useful for disulfide trapping. Furthermore, FA could be used as the primary read-out for induced complex formation. The placement of C180 in the ERRγ DBD motif presented an opportunity for the application of this site-directed approach, based on client FA-tethering to identify novel chemical starting points for PPI enhancers.

For the FA-tethering screen, we used 14−3−3γ, the isoform with the highest affinity for ERRγ DBD (Figure 2b; SI Figure S1) and a fluorescein-labeled ERRγ DBD phosphopeptide. The complex was incubated with 1600 individual disulfide fragments under reducing conditions (250 μM β-mercaptoethanol), at a protein concentration where initially ~25% of the peptide was bound (25% of the maximal FA signal; 1 μM 14−3−3γ). The read-out of this screen was functional stabilization as a result of fragment binding, as observed by an increase in the anisotropy of the labeled phosphopeptide. The free and fully protein-bound peptides were included as controls (Figure 3a). Hit selection was based on an anisotropy value of three standard deviations above the mean of the test compounds (μ + 3σ). On the basis of this, a total of 30 disulfide fragments were selected for further validation experiments.

MOLECULAR MECHANISM OF PPI STABILIZATION

To validate the stabilizing effect observed during the screen, fragments were soaked into cocrystals of 14−3−3σ and the ERRγ DBD phosphopeptide. Only one of the costructures revealed additional electron density, allowing unambiguous modeling of fragment **1** in the continuous density (Figure 3b,c), indicating covalent binding of the fragment to C180 of ERRγ. A side chain flip for Q181 of ERRγ was observed compared to the protein/peptide binary crystal structure, enabling accommodation of the fragment in the pocket. The phenyl group of the fragment engaged the 14−3−3 binding

https://dx.doi.org/10.1021/acschembio.0c00646
ACS Chem. Biol. 2020, 15, 3143−3148

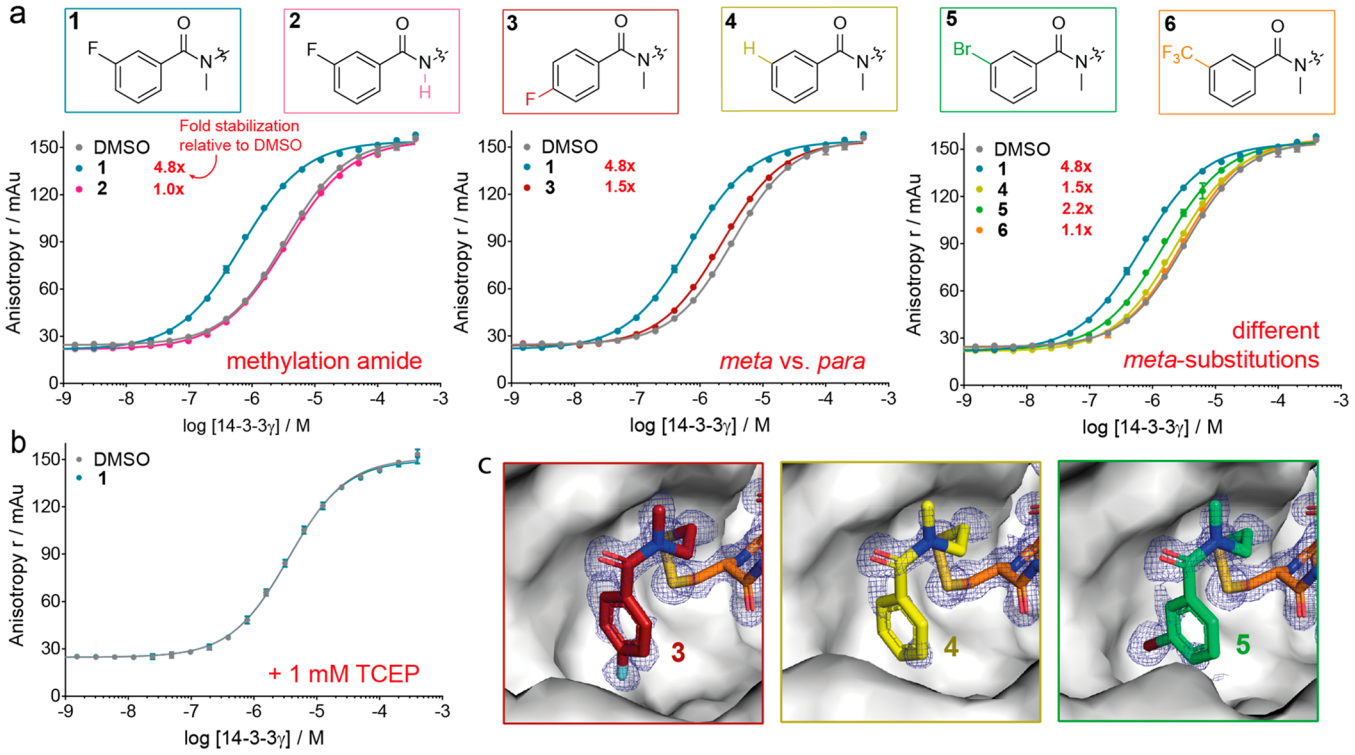

Figure 4. (a) Dose−response anisotropy data for 14−3−3γ titrations to 100 nM fluorescein-labeled ERRγ DBD phosphopeptide in the presence of either DMSO (gray) or 100 μM of fragment **1**−**6** (chemical structures with structural differences compared to **1** given in different colors). (b) Dose−response anisotropy data for 14−3−3γ titrations to 100 nM fluorescein-labeled ERRγ DBD phosphopeptide in the presence of either DMSO or 250 μM of fragment **1**, whereby 1 mM TCEP is added to the assay buffer. (c) Close-up views of ERRγ DBD phosphopeptide (orange sticks) in the 14−3−3 binding groove (white surface) with disulfide-bound fragments **3**, **4**, and **5**. $2F_o - F_c$ electron density maps are contoured at 1σ. PDB: 6Y18, 6XXC, 6XY5.

groove to bury the *meta*-fluorine substitution fully in a hydrophobic cavity. Additionally, the methylated amide was oriented so that the methyl group pointed upward, toward the hydrophobic residues in helix 9 of 14−3−3 that form the "roof" of the pocket.

Interestingly, a crystallographic overlay with the costructure of 14−3−3 bound by an ERα phosphopeptide and 14−3−3σ(C42)-tethered stabilizer reported previously[13] reveals the strikingly similar subpocket engagement by the two distinct fragments (Figure 3d). Whereas both fragments are disulfide-trapped to cysteines, the trapped residue is localized at different sites and on different proteins—C42 of 14−3−3 versus C180 on the ERRγ client peptide. Despite this, a similar orientation of the fragments is observed. Remarkably, even though the halogen substituent is not at the same position (*meta*-fluorine versus *para*-chloro), the phenyl rings are tilted in such a way that the halogens nearly overlap. An additional similarity is the presence of a methyl group pointing upward in the direction of hydrophobic residues on the "roof" of the binding site.

The stabilizing activity of this fragment toward the 14−3−3/ERRγ DBD (C180) protein complex was further studied in a protein titration experiment where 14−3−3γ was titrated against a fixed concentration of fluorescently labeled ERRγ DBD phosphopeptide in the presence of DMSO (control) or increasing concentrations of **1**. Saturating concentrations of **1** resulted in a 5-fold PPI stabilization of the 14−3−3/ERRγ-phosphopeptide complex (Figure 3e).

DISSECTING THE CRUCIAL ELEMENTS FOR STABILIZATION

To investigate which chemical features were important for the stabilization of the 14−3−3/ERRγ phosphopeptide complex, several variants of hit fragment **1** were synthesized. Stabilizing activity of these fragments was analyzed by FA where 14−3−3γ was titrated against a fixed concentration of fluorescein-labeled ERRγ DBD phosphopeptide in the presence of DMSO (control) or 100 μM of disulfide (Figure 4a). The ability of the fragment to stabilize the protein−peptide complex was indicated by the left shift of the binding curve (fold-stabilization relative to DMSO control).

Fragment **2** revealed the significance of the methylated amide as removal of the methyl group destroyed the stabilizing activity of the fragment. This was likely caused by the earlier described interactions between the methyl group of **1** and the hydrophobic amino acids on the "roof" of the 14−3−3 binding groove.

Replacement of *meta*-fluorine substitution with a *para*-fluorine substituent, as in fragment **3**, led to a strong decrease in activity. Given the overlap of halogen positioning between these fragments and fragments from earlier published work (Figure 3d), we expected the exact positioning of the *meta*-fluorine in the 14−3−3 binding groove to be crucial for the stabilization. This was further illustrated by the comparison of fragment **1** to fragments **4**−**6**. When the *meta*-fluorine substituent was removed (fragment **4**), the stabilization fell dramatically. When the *meta*-fluorine was substituted for a bromine substituent (fragment **5**), the fragment retained some stabilization; however, the increase in halogen size seemed to

https://dx.doi.org/10.1021/acschembio.0c00646
ACS Chem. Biol. 2020, 15, 3143−3148

be less favorable for stabilization. This size effect was also apparent in the lack of stabilization by fragment **6**, containing the larger CF_3 substituent. Overall, this concise SAR revealed the impact of small structural changes on the stabilizing effect.

The significance of fragment-peptide disulfide formation for stabilization has been shown by performing the 14−3−3γ titrations in the presence of a large amount of reducing agent (1 mM TCEP). TCEP removed all stabilizing effect by fragment **1** on the PPI as the disulfide formation between the fragment and the peptide was impaired (Figure 4b). The importance of disulfide formation for stabilization was further confirmed as fragment **1** did not stabilize the binding of 14−3−3γ to ERRγ C180S or two other client-derived phosphopeptides that lacked a cysteine (ERα and TAZ, SI Figure S3).

In addition to the FA experiments, fragments were soaked in cocrystals of 14−3−3σ and ERRγ, providing electron densities for three additional fragments (**3**−**5**) with similar binding motifs to those of **1** (Figure 4c). These crystal structures showed weaker electron densities in comparison to fragment **1**. However, the strong electron densities were consistently observed for the disulfide, methylated amide, and halogens, which we postulated were the most crucial elements for 14−3−3/ERRγ PPI stabilization. Interestingly, conclusions drawn from FA data about the importance of halogen positioning and size were confirmed by the crystal structures. Structural overlay of fragment **1** with fragments **3** and **5** shows small ring displacements upward and sideways, respectively (SI Figure S4)

The identification of molecular starting points for the development of PPI stabilizers has been a major hurdle hampering widespread adoption of the paradigm for disease modulation. In our previous work, we showed that disulfide tethering, using an MS based screen, identified fragment molecules that stabilized a 14−3−3 PPI. Herein, we explored a variant of the screen using FA as readout and targeting a native cysteine residue in the client peptide to enhance PPI complex formation. Beginning with a diverse disulfide library, we identified stabilizing chemical matter and validated the screen with a concise SAR, thus illustrating the effectiveness of FA-tethering as a primary screen. In addition to directly selecting for compounds that enhance the PPI, this method has proven itself as a fast, inexpensive, and robust methodology leading to novel chemical matter for PPI modulation.

■ ASSOCIATED CONTENT

Supporting Information

The Supporting Information is available free of charge at https://pubs.acs.org/doi/10.1021/acschembio.0c00646.

FA and ITC 14−3−3/ERRγ motif binding data, cocrystal structure of 14−3−3/ERRγ LBD motif, dose−response curves for FA tethering hits, FA selectivity data, and crystallographic overlay of costructures (Figures S1−S4); experimental methods, synthetic procedures, and compound characterization; XRD data collection and refinement statistics (Table S1) (PDF)

■ AUTHOR INFORMATION

Corresponding Authors

Christian Ottmann − *Laboratory of Chemical Biology, Department of Biomedical Engineering and Institute for Complex Molecular Systems (ICMS), Eindhoven University of Technology, Eindhoven, The Netherlands; Department of Chemistry, University of Duisburg-Essen, Essen, Germany;* orcid.org/0000-0001-7315-0315; Email: c.ottmann@tue.nl

Michelle R. Arkin − *Department of Pharmaceutical Chemistry and Small Molecule Discovery Center (SMDC), University of California, San Francisco, United States;* orcid.org/0000-0002-9366-6770; Email: michelle.arkin@ucsf.edu

Authors

Eline Sijbesma − *Laboratory of Chemical Biology, Department of Biomedical Engineering and Institute for Complex Molecular Systems (ICMS), Eindhoven University of Technology, Eindhoven, The Netherlands*

Bente A. Somsen − *Laboratory of Chemical Biology, Department of Biomedical Engineering and Institute for Complex Molecular Systems (ICMS), Eindhoven University of Technology, Eindhoven, The Netherlands*

Galen P. Miley − *Laboratory of Chemical Biology, Department of Biomedical Engineering and Institute for Complex Molecular Systems (ICMS), Eindhoven University of Technology, Eindhoven, The Netherlands*

Iris A. Leijten-van de Gevel − *Laboratory of Chemical Biology, Department of Biomedical Engineering and Institute for Complex Molecular Systems (ICMS), Eindhoven University of Technology, Eindhoven, The Netherlands*

Luc Brunsveld − *Laboratory of Chemical Biology, Department of Biomedical Engineering and Institute for Complex Molecular Systems (ICMS), Eindhoven University of Technology, Eindhoven, The Netherlands;* orcid.org/0000-0001-5675-511X

Complete contact information is available at: https://pubs.acs.org/10.1021/acschembio.0c00646

Author Contributions

‖These authors contributed equally.

Notes

L.B., M.R.A, and C.O. are founders of Ambagon Therapeutics. L.B. is a member of Ambagon & scientific advisory board, M.R.A. is a director, C.O., E.S., and G.P.M., are employees of Ambagon.

■ ACKNOWLEDGMENTS

We thank the Renslo laboratory for synthesis of the SMDC disulfide library, M. Zhong and G.M. Lee for their help with the FA-tethering screen, and R.J. Neitz and P. Burroughs for sharing synthesis routes and discussing hit optimization. The research described was funded by The Netherlands Organization for Scientific Research (NWO; Gravity Program 024.001.035, Vici grant 016.150.366 and Echo grant 711.017.014) and a Breakthrough Award from the Ono Pharma Foundation.

■ REFERENCES

(1) Scott, D. E., Bayly, A. R., Abell, C., and Skidmore, J. (2016) Small Molecules, Big Targets: Drug Discovery Faces the Protein-Protein Interaction Challenge. *Nat. Rev. Drug Discovery 15* (8), 533−550.

(2) Arkin, M. A., Tang, Y., and Wells, J. A. (2014) Small-Molecule Inhibitors of Protein-Protein Interactions: Progressing Towards the Reality. *Chem. Biol. 21*, 1102−1114.

(3) Dang, C. V., Reddy, E. P., Shokat, K. M., and Soucek, L. (2017) Drugging the "undruggable" Cancer Targets. *Nat. Rev. Cancer 17* (8), 502−508.

(4) Hughes, S. J., and Ciulli, A. (2017) Molecular Recognition of Ternary Complexes: A New Dimension in the Structure-Guided Design of Chemical Degraders. *Essays Biochem. 61* (5), 505−516.
(5) Milroy, L.-G., Bartel, M., Henen, M. A., Leysen, S., Adriaans, J. M. C., Brunsveld, L., Landrieu, I., and Ottmann, C. (2015) Stabilizer-Guided Inhibition of Protein-Protein Interactions. *Angew. Chem., Int. Ed. 54* (52), 15720−15724.
(6) de Weger, V. A., Beijnen, J. H., and Schellens, J. H. M. (2014) Cellular and Clinical Pharmacology of the Taxanes Docetaxel and Paclitaxel - a Review. *Anti-Cancer Drugs 25* (5), 488−494.
(7) Andrei, S. A., Sijbesma, E., Hann, M., Davis, J., O'Mahony, G., Perry, M. W. D., Karawajczyk, A., Eickhoff, J., Brunsveld, L., Doveston, R. G., Milroy, L.-G., and Ottmann, C. (2017) Stabilization of Protein-Protein Interactions in Drug Discovery. *Expert Opin. Drug Discovery 12* (9), 925−940.
(8) Lai, A. C., and Crews, C. M. (2017) Induced Protein Degradation: An Emerging Drug Discovery Paradigm. *Nat. Rev. Drug Discovery 16* (2), 101−114.
(9) Pennington, K. L., Chan, T. Y., Torres, M. P., and Andersen, J. L. (2018) The Dynamic and Stress-Adaptive Signaling Hub of 14−3-3: Emerging Mechanisms of Regulation and Context-Dependent Protein-Protein Interactions. *Oncogene 37* (42), 5587−5604.
(10) Milroy, L.-G., Brunsveld, L., and Ottmann, C. (2013) Stabilization and Inhibition of Protein-Protein Interactions: The 14−3-3 Case Study. *ACS Chem. Biol. 8* (1), 27−35.
(11) Erlanson, D. A., Braisted, A. C., Raphael, D. R., Randal, M., Stroud, R. M., Gordon, E. M., and Wells, J. A. (2000) Site-Directed Ligand Discovery. *Proc. Natl. Acad. Sci. U. S. A. 97* (17), 9367−9372.
(12) Burlingame, M. A., Tom, C. T. M. B., and Renslo, A. R. (2011) Simple One-Pot Synthesis of Disulfide Fragments for Use in Disulfide-Exchange Screening. *ACS Comb. Sci. 13* (3), 205−208.
(13) Sijbesma, E., Hallenbeck, K. K., Leysen, S., de Vink, P. J., Skóra, L., Jahnke, W., Brunsveld, L., Arkin, M. R., and Ottmann, C. (2019) Site-Directed Fragment-Based Screening for the Discovery of Protein-Protein Interaction Stabilizers. *J. Am. Chem. Soc. 141* (8), 3524−3531.
(14) Lodge, J. M., Rettenmaier, T. J., Wells, J. A., Pomerantz, W. C., and Mapp, A. K. (2014) FP Tethering: A Screening Technique to Rapidly Identify Compounds That Disrupt Protein-Protein Interactions. *MedChemComm. 5* (3), 370−375, DOI: 10.1039/C3MD00356F.
(15) Rettenmaier, T. J., Sadowsky, J. D., Thomsen, N. D., Chen, S. C., Doak, A. K., Arkin, M. R., and Wells, J. A. (2014) A Small-Molecule Mimic of a Peptide Docking Motif Inhibits the Protein Kinase PDK1. *Proc. Natl. Acad. Sci. U. S. A. 111* (52), 18590−18595.
(16) Gronemeyer, H., Gustafsson, J.-Å., and Laudet, V. (2004) Principles for Modulation of the Nuclear Receptor Superfamily. *Nat. Rev. Drug Discovery 3* (11), 950−964.
(17) Galliher-Beckley, A. J., Williams, J. G., and Cidlowski, J. A. (2011) Ligand-Independent Phosphorylation of the Glucocorticoid Receptor Integrates Cellular Stress Pathways with Nuclear Receptor Signaling. *Mol. Cell. Biol. 31* (23), 4663−4675.
(18) De Vries-van Leeuwen, I. J., da Costa Pereira, D., Flach, K. D., Piersma, S. R., Haase, C., Bier, D., Yalcin, Z., Michalides, R., Feenstra, K. A., Jimenez, C. R., de Greef, T. F. A., Brunsveld, L., Ottmann, C., Zwart, W., and de Boer, A. H. (2013) Interaction of 14−3-3 Proteins with the Estrogen Receptor Alpha F Domain Provides a Drug Target Interface. *Proc. Natl. Acad. Sci. U. S. A. 110* (22), 8894−8899.
(19) Kim, D.-K., Kim, Y.-H., Hynx, D., Wang, Y., Yang, K.-J., Ryu, D., Kim, K. S., Yoo, E.-K., Kim, J.-S., Koo, S.-H., Lee, I.-K., Chae, H.-Z., Park, J., Lee, C.-H., Biddinger, S. B., Hemmings, B. A., and Choi, H.-S. (2014) PKB/Akt Phosphorylation of ERRγ Contributes to Insulin-Mediated Inhibition of Hepatic Gluconeogenesis. *Diabetologia 57* (12), 2576−2585.
(20) Kim, D.-K., Ryu, D., Koh, M., Lee, M.-W., Lim, D., Kim, M.-J., Kim, Y.-H., Cho, W.-J., Lee, C.-H., Park, S. B., Koo, S.-H., and Choi, H.-S. (2012) Orphan Nuclear Receptor Estrogen-Related Receptor γ (ERRγ) Is Key Regulator of Hepatic Gluconeogenesis. *J. Biol. Chem. 287* (26), 21628−21639.
(21) Madeira, F., Tinti, M., Murugesan, G., Berrett, E., Stafford, M., Toth, R., Cole, C., MacKintosh, C., and Barton, G. J. (2015) 14−3-3-Pred: Improved Methods to Predict 14−3-3-Binding Phosphopeptides. *Bioinformatics 31* (14), 2276−2283.
(22) Gearhart, M. D., Holmbeck, S. M. A., Evans, R. M., Dyson, H. J., and Wright, P. E. (2003) Monomeric Complex of Human Orphan Estrogen Related Receptor-2 with DNA: A Pseudo-Dimer Interface Mediates Extended Half-Site Recognition. *J. Mol. Biol. 327* (4), 819−832.

https://dx.doi.org/10.1021/acschembio.0c00646
ACS Chem. Biol. 2020, 15, 3143−3148